The reptiles of Tinhosa Grande islet (Gulf of Guinea): A taxonomic update and the role of Quaternary sea level fluctuations in their diversification

Luis MP Ceríaco , Justin Bernstein , Ana C Sousa , Mariana P Marques , Aaron M Bauer & Sietze J Norder

View supplementary material

Published online: 30 Nov 2020.

Submit your article to this journal

View related articles

View Crossmark data

Check for updates

The reptiles of Tinhosa Grande islet (Gulf of Guinea): A taxonomic update and the role of Quaternary sea level fluctuations in their diversification

Luis MP Ceríaco [a,b], Justin Bernstein [c], Ana C Sousa [d], Mariana P Marques [b,e], Aaron M Bauer [f] and Sietze J Norder [g]

aMuseu de História Natural e da Ciência, Universidade do Porto, Porto, Portugal; bDepartamento de Zoologia e Antropologia (Museu Bocage), Museu Nacional de História Natural e da Ciência, Universidade de Lisboa, Lisbon, Portugal; cDepartment of Biological Sciences, Rutgers University-Newark, Newark, USA; dDepartamento de Biologia, Universidade de Évora, Évora, Portuga; eResearch Center in Biodiversity and Genetic Resources (CIBIO), InBIO, University of Porto, Porto, Portugal; fDepartment of Biology and Center for Biodiversity and Ecosystem Stewardship, Villanova University, Pennsylvania, USA; gLeiden University Centre for Linguistics, Leiden, The Netherlands

ABSTRACT

The reptile fauna of Tinhosa Grande islet, Gulf of Guinea, comprises an endemic skink, *Trachylepis adamastor*, and an unidentified species of gecko of the genus *Hemidactylus*. Until recently, no molecular data were available for either species, impeding their phylogenetic placement. However, due to several synapomorphic characters, it was suggested that the Tinhosa Grande population would be related to the congeners of the neighbouring islands of Príncipe and São Tomé. In a recent survey of Tinhosa Grande islet we collected fresh material of both species, allowing us to examine their phylogenetic relationships to the other members of their respective genera occurring on the neighbouring islands using multigene Bayesian and maximum likelihood analyses. In contrast with the morphological results and previous taxonomic allocations, our molecular results suggest that both *T. adamastor* and the unidentified *Hemidactylus* sp. are conspecific with their Príncipe counterparts, *Trachylepis principensis* and *Hemidactylus principensis*. While today Tinhosa and Príncipe differ strongly in their environmental conditions, we show that the islands have been repeatedly merged into a single landmass as a result of Quaternary sea level fluctuations. We suggest that the repeated fusion of the islands during low sea levels could have impeded the phylogenetic divergence of both populations, while contrasting habitats might have simultaneously promoted some morphological differences.

Introduction

The herpetofauna of the insular nation of São Tomé and Príncipe, Gulf of Guinea, has been the topic of considerable research in recent years. Since 2007, several new species of

---

African Journal of Herpetology is co-published by NISC Pty (Ltd) and Informa Limited (trading as Taylor & Francis Group)

amphibians and reptiles have been described for the country. These include a puddle-frog, *Phrynobatrachus leveleve* Uyeda, Drewes and Zimkus, 2007, a snake-eyed-skink, *Panaspis thomensis* Ceríaco, Soares, Marques et al. 2017, and a cobra, *Naja peroescobari* Ceríaco, Marques, Schmitz and Bauer, 2017, all endemic to São Tomé, a reed-frog, *Hyperolius drewesi* Bell, 2016, and a house gecko, *Hemidactylus principensis* Miller, Sellas and Drewes, 2012, both endemic to Príncipe; and three new skinks of the genus *Trachylepis*, *T. adamastor* Ceríaco, 2015, *T. principensis* Ceríaco, Marques and Bauer, 2016, and *T. thomensis* Ceríaco, Marques and Bauer, 2016, endemic to the islet of Tinhosa Grand, Príncipe, and São Tomé, respectively.

All of these recent descriptions have been based on a combination of molecular and morphological data, with the exception of *T. adamastor*. This species, endemic to the Tinhosa Grande, a 20.5 ha islet that lies approximately 20 km off the coast of Príncipe island, was described solely based on morphological data from historical specimens. Due to long-term preservation in formalin, all attempts to extract molecular data from the original type series were unsuccessful, and, given the lack of any fresh material, it was impossible to place the newly described taxon in the existing phylogenies. Nonetheless, given the morphological similarities of *T. adamastor* to its congeners of the surrounding islands, at the time still considered as part of the *Trachylepis maculilabris* (Gray, 1845) species complex, Ceríaco (2015) suggested that this Tinhosa Grande endemic skink would be associated with that species complex. A subsequent revision of the genus *Trachylepis* of the oceanic islands of the Gulf of Guinea shed some additional light on the taxonomic identity and phylogenetic relationships of the island species. Based on a combination of morphological and molecular data, Ceríaco et al. (2016) provided evidence that the *T.* cf. *maculilabris* populations of São Tomé and Príncipe were, in fact, two different species, each endemic to its respective island. Additionally, these authors provided evidence for the presence of a non-endemic species on Príncipe island, *Trachylepis affinis* (Gray, 1838), and reviewed the identity of the Annobon island endemic *Trachylepis ozorii* (Bocage, 1893). In this revision, the authors revisited the identity and taxonomic status of *T. adamastor* and compared its morphology to that of the newly described species of São Tomé and Príncipe. As no molecular data were available at the time and given the consistent morphological differences between the three taxa, Ceríaco et al. (2016, 2018) continued to consider *T. adamastor* as a valid species. A recent species-level phylogeny of the genus by Weinell et al. (2019) provided new data on the phylogenetic relationship of some Gulf of Guinea Oceanic islands endemic species, namely *T. principensis*, *T. thomensis* and *T. ozorii*, but molecular data for *T. adamastor* was still not available.

In recent expeditions to Tinhosa Grande we collected new specimens of *T. adamastor*, as well as specimens of an unidentified species of *Hemidactylus* gecko. The newly collected material allows us to resolve the taxonomic identity of the Tinhosa Grande reptiles, as well as to understand their phylogenetic affinities. This is especially important as it may provide novel data about the role of past sea level fluctuations, and subsequent repeated cycles of island fusion and fission, in shaping the biodiversity of these islands. The Gulf of Guinea islands differ greatly in terms of their ontogeny and bathymetry (Lee et al. 1994), and the palaeogeography of each of these islands likely had a unique response to fluctuations in sea level. It has been widely recognised that glacial-interglacial sea-level fluctuations have shaped insular biodiversity and diversification across the globe by repeatedly

connecting and disconnecting populations on landmasses (Woodruff 2010; de Bruyn et al. 2014; Rijsdijk et al. 2014; Fernández-Palacios et al. 2016; Fernández-Palacios 2016; Weigelt et al. 2016; Norder et al. 2019). During periods of low sea level, increased geographic connectivity might promote gene flow and as suchlimit divergence (Heaney et al. 2005; Ali and Aitchison 2014; Papadopoulou and Knowles 2017), although it should be noted that even when islands are physically connected, environmental differences between them could still form a dispersal barrier for some species (Bell et al. 2017; Flantua et al. 2020). In contrast, the separation of islands during periods of high sea level might promote genetic and phenotypic divergence in allopatry, leading to reproductive isolation (Gillespie and Roderick 2014). For example, Late Pleistocene marine incursions that separated Bioko from the African continent likely promoted the genetic and phenotypic divergence of frogs on Bioko island (Bell et al. 2017; Charles et al. 2018). Similarly, it is possible that the fission of Príncipe and Tinhosa Grande islet during interglacial high sea levels may have contributed to the isolation and subsequent speciation of the reptiles occurring on the islands; alternatively their fusion during glacial lows may have prevented this process.

Here, we combine a phylogenetic analysis incorporating recently obtained molecular data with a reconstruction of sea-level driven changes in palaeogeography of islands in the Gulf of Guinea in order to provide a better understanding of the taxonomy and phylogenetic affinities of the Tinhosa Grande reptiles, as well as to gather insights into the role of repeated island fusion and fission in morphological and phylogenetic divergence.

Materials and methods

Morphological methods

Specimens collected for this study were euthanised, preserved in 10% buffered formalin in the field, and transferred to 70% ethanol for storage at the conclusion of the expedition. Liver tissue was removed before formalin fixation, preserved in RNA later, and transferred to 95% ethanol for long-term storage. For mensural and meristic comparisons we examined 67 specimens of *Trachylepis* and *Hemidactylus* species (including the type series of *T. adamastor*, *T. principensis* and *T. thomensis*) deposited in the California Academy of Sciences (CAS; San Francisco, U.S.A.), the Instituto de Investigação Científica Tropical (IICT; Lisboa, Portugal), and the Museu Nacional de História Natural e da Ciência (MUHNAC/MB; Lisboa, Portugal). All specimens examined are listed in Supplementary Table 1. Information on morphological characters of species and/or type material that could not be examined, as well as supplemental data for *Hemidactylus* species, was obtained from the relevant literature (e.g. Miller et al. 2012). For *Trachylepis*, morphological analyses followed the procedures of Ceríaco (2015) and Ceríaco et al. (2016). The following characters were measured with a digital calliper (0.01 mm): snout-vent length (SVL), from the snout to the vent; tail length (TL), from cloaca to tip of tail, measured only in specimens with complete, original tails; head width (HW); head length (HL), from tip of snout to anterior tympanum border; head height (HH), from the base of the maxilla to the top of head; eye-snout distance (ES), from the front of the eye to the tip of the snout; eye-nostril distance (EN), from the front of the eye to the nostril; internostril distance (IN), minimum distance between the nostrils; number of scale rows at midbody (MSR); number of scales dorsally (SAD), from the nuchal (excluded from count) to base of the tail; number of scales ventrally (SAV), from the

mental (excluded from count) to the anal plate (excluded); number of subdigital lamellae under Finger-IV (LUFF); number of subdigital lamellae under Toe-IV (LUFT); number of supra-labials (SL), with those widened in subocular position indicated between brackets; number of supraciliaries (SC); number of supraoculars (SO); number of nuchal scales (NS); number of keels on dorsal scales (KDS); kind of contact between parietals (CP); kind of contact between frontoparietals (CFP); kind of contact between supranasals (CSN); kind of contact between prefrontals (CPF). For *Hemidactylus*, morphological analyses followed the procedures of Miller et al. (2012). The following characters were measured: snout-vent length (SVL; from tip of snout to vent), trunk length (TRL; distance from axilla to groin measured from posterior edge of forelimb insertion to anterior edge of hind limb insertion), body width (BW; maximum width of body), crus length (CL; from base of heel to knee); tail length (TL; from vent to tip of tail), tail width (TW; measured at widest point of tail); head length (HL; distance between retroarticular process of jaw and snout-tip), head width (HW; maximum width of head), head height (HH; maximum height of head, from occiput to underside of jaws), forearm length (FL; from base of palm to elbow); orbital diameter (OD; greatest diameter of orbit), nares to eye distance (NE; distance between anterior most point of eye and nostril), snout to eye distance (SE; distance between anterior most point of eye and tip of snout), eye to ear distance (EE; distance from anterior edge of ear opening to posterior corner of eye), internarial distance (IN; distance between nares), interorbital distance (IO; shortest distance between left and right supraciliary scale rows), longitudinal rows of enlarged dorsal tubercles at midbody (DTR) and number of precloacal pores.

Molecular methods

Fresh tissues of *T. adamastor* and *Hemidactylus* sp. were collected on Tinhosa Grande, allowing us to assess their relationships with the fauna of surrounding islands and main-land Africa. We extracted DNA using a previously described ethanol precipitation protocol (Aljanabi and Martinez 1997). We used polymerase chain reaction (PCR) to amplify the two mitochondrial genes (16s, ND2) and one nuclear (RAG-1) gene for five *Trachylepis*: *T. adamastor*, *T. principensis*, *T. thomensis*, *T. maculilabris* (continental Africa) and *T. affinis* (Príncipe Island, used as outgroup), and four *Hemidactylus*: *H.* sp. from Tinhosa Grande, *H. greeffii*, *H. principensis* and *H. mabouia* (used as outgroup) (Supplementary Table 1). Primers used for amplification of 16s (16sA, 16sB), ND2 (Metf1, CO1R1, CO1R8, L5002), and RAG-1 (RAG-1 F700, RAG-1R700, RAG1skinkF370, RAG1skinkF1200) were obtained from previous studies (16s: Palumbi et al. 1991; ND2: Macey et al. 1997; Weisrock et al. 2001; RAG-1: Bauer et al. 2007; Portik et al. 2010). Genes were sequenced on an ABI 3730 xl DNA analyser and contiguous sequences were aligned in Geneious v. 6.1 (Kearse et al. 2012) and edited manually. Because no heterozygotes were found in the nuclear (RAG-1) chromatograms, we did not phase these data. We inferred the species tree using 16S, ND2, and RAG1 in a coalescent framework using BEAST2 (Bouckaert et al. 2014) and ran it for 100 million generations, sampling every 10,000 generations under a Yule model of speciation. We used Tracer v 1.7 (Rambaut et al. 2018) to check for con-vergence of the analysis (10% burn-in) and to check all estimated sample size (ESS) values. All trees from the analysis were combined to obtain a maximum clade credibility tree using TreeAnnotator. All Bayesian posterior probabilities values ≥ 0.95 are considered strongly supported. Bayesian model selection for species tree analysis was performed

on the partitioned datasets using bModelTest using the TransitionTransversionSplit option as implemented in BEAST2 (Bouckaert and Drummond 2017). Mean uncorrected pairwise distances between species were obtained using MEGA v7 (Kumar et al. 2016). To quantitatively support phylogenetic interpretations of species boundaries, we ran Markov Chain Monte Carlo (MCMC) sampling with a multirate Poisson Tree Processes (mPTP) for species delimitation on all individual gene trees. The mPTP method delimits species while taking phylogeny into account and does not require any input similarity threshold (Kapli et al. 2017). We performed two MCMC runs using a single-threshold for 500 million generations and a 10% burn-in.

Palaeogeographic reconstructions

To reconstruct changes in palaeogeography of the Gulf of Guinea Islands (Bioko, Príncipe, São Tomé and Annobon) and surrounding islets (Tinhosa Grande) resulting from past sea-level fluctuations, we used data from the Palaeo-Islands and Archipelago Configuration (PIAC) database (Norder et al. 2018). Because no regional sea-level curve is available, we compared the palaeogeography as reconstructed using available global sea-level curves (Cutler et al. 2003; Lambeck et al. 2014). We then cropped a global Digital Elevation Model (including bathymetry) to the extent of the Gulf of Guinea (GEBCO 2014) to determine the threshold sea level at which the repetitive fusion and fission of Príncipe and Tinhosa Grande occurred. Finally, we used available data (Bintanja et al. 2005) to determine the duration of the period over which sea levels were below this threshold during the past 1 Myr. With this approach, we were able to determine during which time intervals and how frequently Príncipe and Tinhosa Grande were connected and separated.

Results

Morphology

Comparisons between *T. adamastor* from Tinhosa Grande islet, *T. principensis* from Príncipe island and *T. thomensis* from São Tomé island are presented in Table 1. Comparisons between *Hemidactylus* sp. from Tinhosa Grande islet, *H. principensis* from Príncipe Island and *H. greeffii* from São Tomé Island are presented in Table 2. As noted by Ceríaco (2015) and Ceríaco et al. (2016), *T. adamastor* differs from *T. principensis* and *T. thomensis* in several characters, including size (Max SVL for *T. adamastor* 112.04 mm, versus 88.30 in *T. principensis*, 92.10 in *T. thomensis*), the number of lamellae under the fourth toe (13–20 for *T. adamastor*, versus 20–23 in *T. principensis*, 15–20 in *T. thomensis*) and coloration pattern (dorsum homogenous dark-brown *T. adamastor*, versus brown in *T. principensis*, brownish, with some dark and white speckles in *T. thomensis* Table 1). No significant differences were found between the Tinhosa Grande *Hemidactylus* and *H. principensis* (Table 2).

Genetic analyses

In the *Trachylepis* species tree, four groups were recovered: *T. affinis* (outgroup), *T. maculilabris*, *T. thomensis*, and *T. principensis* + *T. adamastor* (Figure 1). The *Hemidactylus*

Table 1. General comparison between *Trachylepis* species from Tinhosa Grande islet, Príncipe and São Tomé Islands. Data presented as 'min-max (mean ± standard deviation)'. Abbreviations are the same as those described in Materials and methods.

	T. adamastor (*n* = 22) Tinhosa Grande islet	*T. principensis* (*n* = 13) Príncipe Island	*T. thomensis* (*n* = 13) São Tomé Island
SVL (mm)	72.00–112.04 (103.96 ± 8.02)	69.50–88.30 (81.75 ± 5.55)	74.00–92.10 (81.88 ± 6.54)
TL	23.00–175.64 (114.56 ± 36.43)	140.00–184.10 (157.06 ± 15.34)	116.3–180.00 (137.65 ± 17.14)
HW	9.49–15.85 (13.45 ± 1.56)	8.80–13.10 (10.87 ± 1.13)	9.00–13.5 (11.18 ± 1.25)
HL	12.15–22.37 (18.09 ± 1.96)	14.50–19.90 (17.56 ± 1.36)	15.30–21.00 (17.46 ± 1.58)
HH	5.44–13.00 (9.79 ± 1.57)	6.60–9.30 (8.12 ± 0.75)	6.30–11.10 (8.77 ± 1.48)
IN	2.50–4.18 (3.52 ± 0.46)	1.90–2.80 (2.38 ± 0.26)	1.50–3.70 (2.69 ± 0.60)
EN	4.34–7.42 (6.39 ± 0.73)	3.30–6.10 (4.87 ± 0.67)	3.90–6.20 (4.92 ± 0.80)
ES	6.71–10.08 (8.91 ± 0.99)	6.00–7.60 (6.82 ± 0.55)	6.10–8.80 (7.02 ± 0.85)
HL/SVL (%)	15.50–20.63 (17.40 ± 1.24)	20.10–24.10 (21.50 ± 1.44)	19.20–24.20 (21.35 ± 1.45)
ES/HL (%)	39.24–57.65 (49.65 ± 6.41)	36.10–41.60 (38.83 ± 1.88)	37.10–49.30 (40.22 ± 3.09)
HH/HL (%)	43.87–70.47 (54.10 ± 6.97)	41.80–81.40 (57.69 ± 16.18)	41.30–62.00 (49.91 ± 5.32)
HW/HL (%)	58.15–87.09 (74.64 ± 7.61)	55.30–65.90 (61.72 ± 2.75)	56.60–78.90 (63.91 ± 5.24)
TL/SVL (%)	21.30–164.95 (111.19 ± 34.45)	167.10–228.10 (198.44 ± 22.73)	145.20–205.10 (167.10 ± 21.27)
LUFT	13–20	20–23	15–20
LUFF	15–17	16–18	15–22
MSR	31–35	31–33	31–35
SAD	48–54	47–51	55–59
SAV	56–66	57–64	58–64
KDS	3–6	5–6	4–6
CP	Always in contact. or in contact in a single point	Always in contact. or in contact in a single point	Usually in contact. or in contact in a single point
CFP	Always in contact	Always in contact	Always in contact
CPF	Variable	Variable	Variable
CSN	Always in contact forming a suture	Always in contact	Always in contact
Coloration	In preservative. the background color of the flanks and the upper side of head. neck. Back, legs and tail is very dark-brown, with many subtle white speckles on the dorsum starting on the neck and running through the entire dorsum to the base of tail. A very subtle darker lateral band, starting on the extremities of the nuchals continues until the arm insertion. Lateral area of the body greyish, with some brown stains. Venter uniformly whitish. Supralabials present a whithish area on the base. black on the top.	Back uniformly brownish and belly light bluish on alcohol preserved specimens. and bluish to greenish in life specimens.	Back brownish. with some dark and white speckles and belly light orange-yellow in alcohol preserved specimens, pinkish-yellow in live specimens. A thin horizontal line composed by approximately seven to eight white speckles from the back of the eye to the top of the tympanum.

species tree recovered three groups: *H. mabouia* (outgroup), *H. greeffii* and *H. principensis* + *H.* sp. from Tinhosa Grande (Figure 2). All nodes in both species trees were strongly supported with the exception of the node subtending *T. thomensis* and *T. principensis* + *T. adamastor*, as well as the node grouping all of the in-group *Trachylepis* (Figure 1). Uncorrected pairwise distances of the three genes used for each species show high species-level divergence values between the different species pairs from São Tomé and Príncipe (*T. principensis/T. thomensis*, *H. greeffii/H. principensis*; Tables 3 and 4), as well between the island species and those of the mainland or respective outgroups. However, very low divergence values (below the typical interspecific divergences among sister species in

Table 2. General comparison between *Hemidactylus* species from Tinhosa Grande islet, Príncipe and São Tomé Islands. Data presented as 'min-max (mean ± standard deviation)'. Abbreviations are the same as those described in Materials and methods.

	H. sp. (*n* = 8) Tinhosa Grande islet	*H. principensis* (*n* = 8) Príncipe Island	*H. greeffii* (*n* = 3) São Tomé Island
SVL (mm)	26.73–61.05 (39.14 ± 11.81)	48.07–60.73 (55.23 ± 4.21)	59.57–74.10 (66.25 ± 7.33)
TRL	10.84–26.52 (16.02 ± 5.50)	17.19–24.29 (21.91 ± 2.78)	24.52–26.29 (25.67 ± 1.00)
BW	4.84–15.46 (8.31 ± 3.66)	7.12–13.74 (11.32 ± 2.00)	12.79–14.53 (13.56 ± 0.89)
CL	5.55–11.38 (8.01 ± 2.04)	10.95–14.56 (12.82 ± 1.32)	15.23–17.40 (15.98 ± 1.23)
TL	8.10–32.12 (22.59 ± 10.06)	21.58–70.03 (53.02 ± 16.64)	47.67–92.47 (70.12 ± 22.40)
TW	2.08–8.04 (3.92 ± 2.03)	5.13–7.83 (5.86 ± 1.00)	5.64–7.56 (6.44 ± 1.00)
HL	6.87–14.20 (9.44 ± 2.52)	11.49–13.86 (12.82 ± 0.76)	13.94–15.80 (14.77 ± 0.95)
HW	5.54–13.01 (8.05 ± 2.35)	9.05–12.08 (10.50 ± 0.94)	11.81–13.86 (12.49 ± 1.18)
HH	3.05–7.38 (4.53 ± 1.39)	4.86–6.30 (5.57 ± 0.50)	6.85–7.56 (7.24 ± 0.36)
FL	3.00–7.75 (4.63 ± 1.65)	5.43–7.79 (6.68 ± 0.70)	8.01–10.29 (9.17 ± 1.14)
OD	2.03–3.44 (2.51 ± 0.47)	2.26–3.45 (2.84 ± 0.39)	3.87–4.47 (4.07 ± 0.35)
NE	2.67–5.67 (3.59 ± 1.04)	3.60–5.66 (4.67 ± 0.66)	5.19–6.93 (5.99 ± 0.88)
SE	3.62–7.30 (4.86 ± 1.29)	5.48–7.51 (6.64 ± 0.68)	7.31–8.39 (7.69 ± 0.60)
EE	2.66–5.34 (3.80 ± 0.97)	4.37–5.95 (4.87 ± 0.52)	4.55–5.52 (5.19 ± 0.55)
IN	1.56–2.78 (1.97 ± 0.42)	1.57–2.07 (1.94 ± 0.17)	2.33–2.80 (2.50 ± 0.26)
IO	3.16–6.91 (4.55 ± 1.21)	5.00–6.33 (5.87 ± 0.41)	6.00–7.58 (6.99 ± 0.86)
Precloacal pores (in males)	26–34	26–39	42–48
Longitudinal rows of tubercles	17–21	18–21	17–21
Divided lamellae on 3rd finger (left hand)	7–8	7–8	9–9
Divided lamellae on 3rd finger (right hand)	7–8	7–8	9–10
Divided lamellae on 3rd finger (left foot)	7–8	8–9	10–11
Divided lamellae on 3rd finger (right foot)	7–8	8–9	10–11
Supralabials left side	9–12	10–12	10–11
Supralabials right side	9–12	10–13	10–11
Infralabials left side	8–9	9–10	9–9
Infralabials right side	8–10	8–11	8–9

these genera, see Ceríaco et al. 2016, 2020) are observed between Príncipe and Tinhosa Grande populations/species (Tables 3 and 4).

The mPTP species delimitation analysis recovered *H. mabouia* and *H. greeffii* as distinct species in the 16s and ND2 gene trees (See Supplementary material). The Tinhosa populations of *Hemidactylus* were grouped with *H. principensis* (i.e. synonymous), in the mitochondrial trees. All taxa of *Hemidactylus* were considered one species in the RAG-1 tree (See Supplementary material). Both the 16s and ND2 *Trachylepis* trees delimited all described species as distinct species with the exception of *T. adamastor* and *T. principensis*, which were considered the same species by the analysis (See Supplementary material). Delimitation based on the RAG-1 *Trachylepis* tree grouped *T. adamastor*, *T. principensis*, *T. thomensis*, and *T. maculilabris* as one species, and *T. affinis* as a second species (See Supplementary material).

Palaeogeographic reconstructions

The four present-day Gulf of Guinea Islands show distinctive area changes in response to eustatic sea-level fluctuations (Figures 3, 4, and 5). During the exceptionally low sea level of the Last Glacial Maximum (LGM), Annobón was five times its present size, and

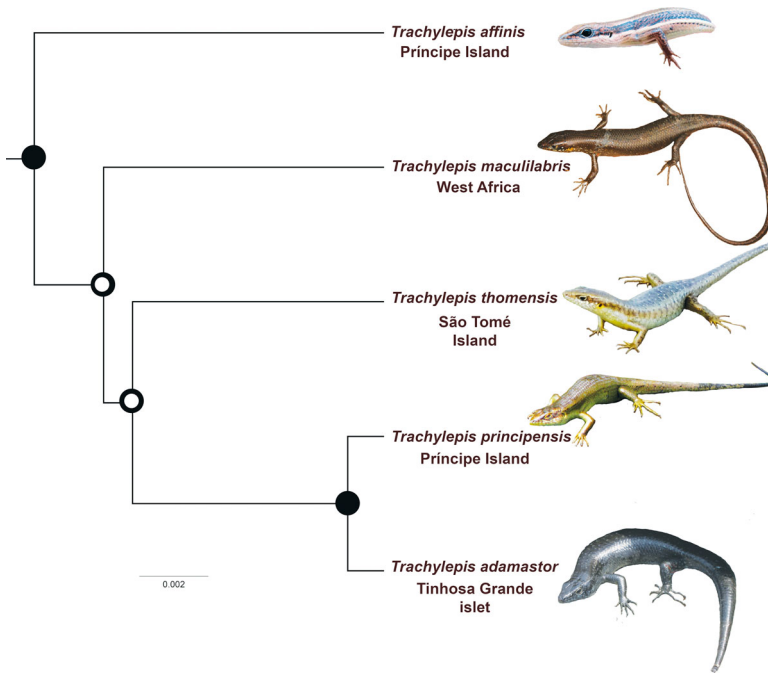**Figure 1.** Maximum clade credibility tree of *Trachylepis* of São Tomé, Príncipe and surrounding Islets. Open and filled nodes represent low (≤0.94) and high (≥0.95) Bayesian posterior probabilities, respectively.
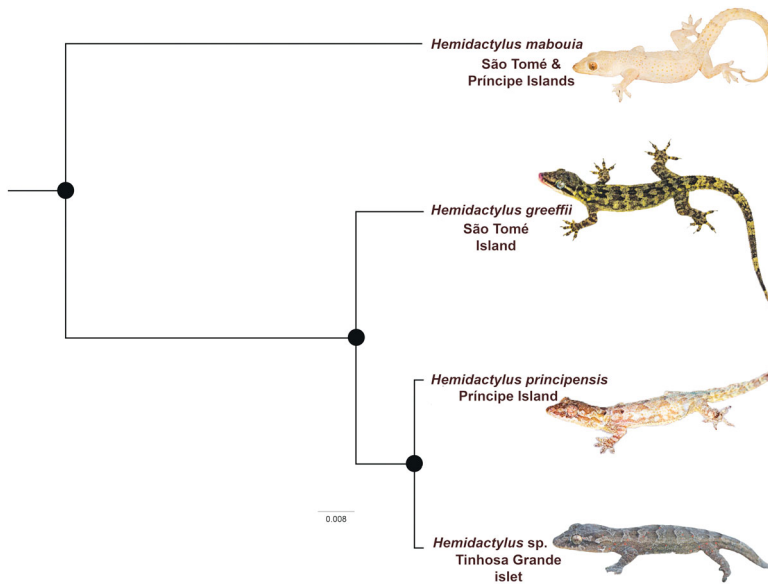

Figure 2. Maximum clade credibility tree of *Hemidactylus* of São Tomé, Príncipe and surrounding Islets. Filled nodes represent high (≥0.95) Bayesian posterior probabilities.

Table 3. Mean uncorrected pairwise distances (in %) between the compared *Trachylepis* species, for mitochondrial and nuclear genes. Grey-shaded boxes represent mean intraspecific gene distances. Parenthetical numbers indicate specimen sample sizes for the respective taxa.

		Trachylepis maculilabris	*Trachylepis affinis*	*Trachylepis thomensis*	*Trachylepis adamastor*	*Trachylepis principensis*
Trachylepis maculilabris	16S (33)	0.4	10.3	7.3	6.7	7.0
	ND2 (17)	0	25.9	20.2	20.8	21.1
	RAG1 (18)	0.1	2.7	0.9	1.1	1.1
Trachylepis affinis	16S (7)	10.3	0.4	9.4	10.7	10.3
	ND2 (2)	25.9	0.2	23.9	23.2	23.4
	RAG1 (3)	2.7	0.2	3.1	3.4	3.3
Trachylepis thomensis	16S (19)	7.3	9.4	0.1	6.6	6.7
	ND2 (2)	20.2	23.9	0	19.2	19.5
	RAG1 (3)	0.9	3.1	0	1.4	1.4
Trachylepis adamastor	16S (14)	6.7	10.7	6.6	0	0.4
	ND2 (4)	20.8	23.2	19.2	0.4	0.4
	RAG1 (3)	1.1	3.4	1.4	0.6	0.6
Trachylepis principensis	16S (5)	7.0	10.3	6.7	0.4	0.1
	ND2 (5)	21.1	23.4	19.5	0.4	0.5
	RAG1 (3)	1.1	3.3	1.4	0.6	0.2

Bioko was connected to continental Africa. Area change of Príncipe has been much more drastic compared to São Tomé. While today São Tomé is six times the size of Príncipe, during periods of extremely low sea levels they both approximated 1 400 km^2 (Figure 3). Repeated island fusion and fission took place between 71 m and 70 m below the present-day sea level (Figure 4). Regardless of which sea-level curve is used (Cutler et al. 2003; Lambeck et al. 2014), at the resolution of 1 km^2 considered here, the timing of the most recent separation is identical; Príncipe and the Tinhosa Islets were still connected at 13 ka, but separated at 12 ka. Over the past 1 Myr, Príncipe and the Tinhosa Islets were connected 14 times (Figure 5) and were merged into a single palaeo-island for 42% of the time over the past 1 Myr.

Table 4. Mean uncorrected pairwise distances (in%) between the compared *Hemidactylus* species, for mitochondrial and nuclear genes. Grey-shaded boxes represent mean intraspecific gene distances. Parenthetical numbers indicate specimen sample sizes for the respective taxa. Taxa represented by only one specimen do not have calculated intraspecific distances (NA).

		Hemidactylus mabouia	*Hemidactylus greeffii*	*Hemidactylus principensis*	*Hemidactylus* sp. (Tinhosa)
Hemidactylus mabouia	16S (4)	0	13.8	13.0	13.0
	ND2 (6)	0	29.6	33.6	32.4
	RAG1 (3)	0	3.9	3.9	4.4
Hemidactylus greeffii	16S (3)	13.8	0	2.6	2.6
	ND2 (3)	29.6	0.1	8.4	7.4
	RAG1 (1)	3.9	NA	0.3	0.9
Hemidactylus principensis	16S (8)	13.0	2.6	0.2	0.3
	ND2 (8)	33.6	8.4	0.6	1.2
	RAG1 (1)	3.9	0.3	NA	0.7
Hemidactylus sp. (Tinhosa)	16S (7)	13.0	2.6	0.3	0.2
	ND2 (7)	32.4	7.4	1.2	0.2
	RAG1 (1)	4.4	0.9	0.7	NA

Discussion

Our results corroborate that both *T. adamastor* and the *Hemidactylus* sp. from Tinhosa islet belong to the same species complex of their counterparts in Príncipe island as already been proposed by Ceríaco (2015) and Ceríaco et al. (2016), suggesting, however, that contrary to what was assumed, the Tinhosa Grande populations are not endemic to the islet, but rather are isolated populations of Príncipe taxa. Although the absence of fossil data precludes a precise calibration of evolutionary rates, our results support a very recent divergence between Tinhosa and Principe populations for both genera. Considering
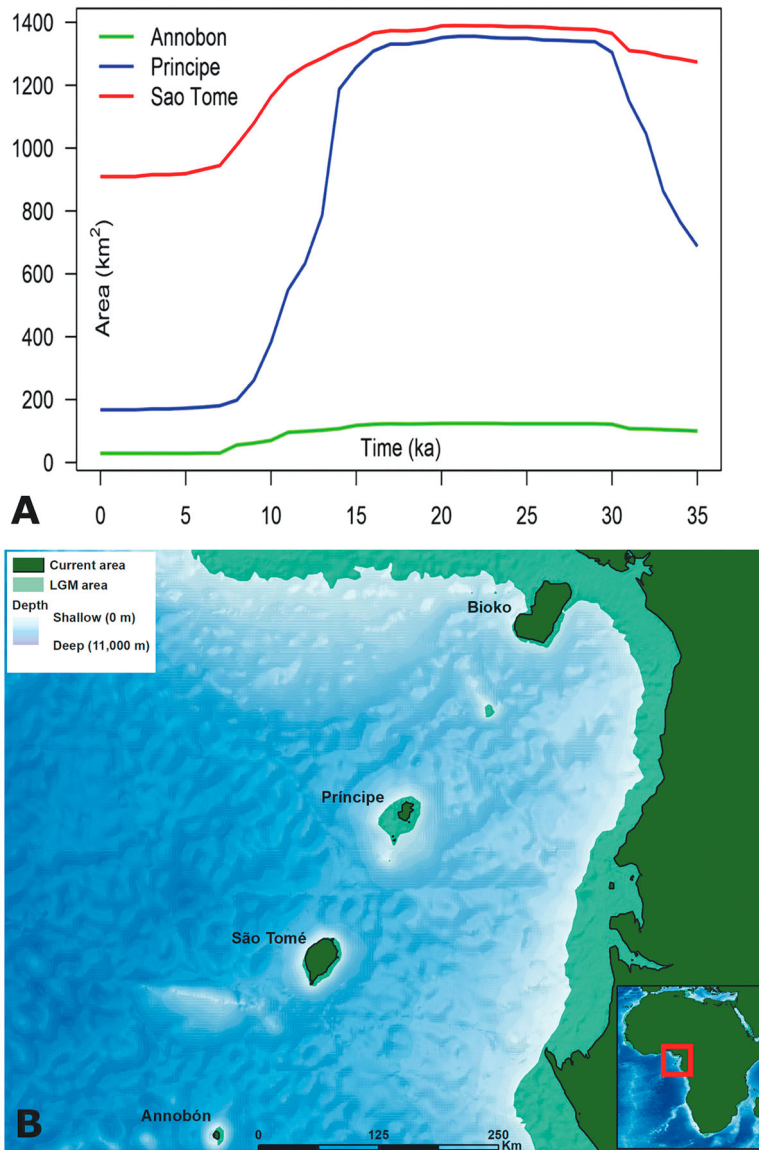

Figure 3. (A) Area change curves of Príncipe, São Tomé, and Annobón; (B) Area of islands today, and extreme area at the last glacial maximum (LGM, approximately 21 ka).
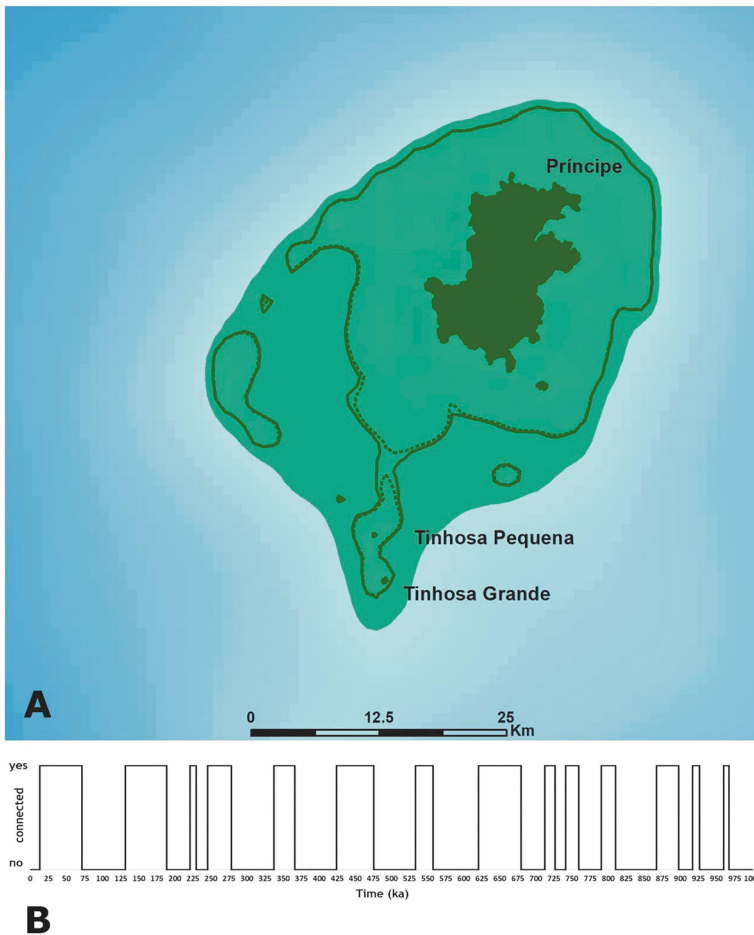
Figure 4. (A) Palaeo-configuration of Príncipe and Tinhosa Grande at the threshold between −71 m msl (solid line) and −70 m msl (dotted line); (B) Number of occurrences and duration of Príncipe and Tinhosa Grande connectivity over the past 1 Ma.

estimated rates of evolution for skinks (see Smith 2007), the level of mitochondrial divergence between the Tinhosa Grande and Príncipe populations seems to roughly agree with the inferred Quaternary fusion of the island and islet when the global sea-level first fell below the critical level of −71 m msl (Bintanja and van de Wal 2008). This initial connection, potentially allowing for the colonization of Tinhosa from Príncipe, was followed by repetitive cycles of island separation and connectedness. However, because the amplitude of sea-level fluctuations has increased over the past 3 Myr (Bintanja and van de Wal 2008), both the frequency and duration of island connection has gradually increased towards the present (Figure 5). The levels of divergence for ND2 between Tinhosa and Principe *Hemidactylus* are about three times that of the *Trachylepis* species, but it has been observed that mitochondrial evolutionary rates in geckos are generally much greater than other squamates (Jesus et al. 2005; Miller et al. 2012). These results are in accordance with other cases that found that populations on islands that were merged during lower sea-levels showed lower genetic divergence than populations

Figure 5. Habitat at Tinhosa Grande (top) and Príncipe Island (below). Photos by Luis MP Ceríaco.

on islands that were never connected (Heaney et al. 2005; Ai and Aitchison 2014; Papado-poulou and Knowles 2017). Analyses are currently being conducted to better understand and provide approximate timings for the speciation events for most of the squamate species of the Gulf of Guinea Oceanic islands, which will also contribute to fine-tune the Tinhosa Grande and Príncipe populations isolation events (Ceríaco et al. unpubl. data).

Based on our molecular and species delimitation results, the Tinhosa Grande skinks and geckos are conspecific with their Príncipe counterparts. The palaeogeographic reconstructions corroborate the phylogenetic results and low interisland genetic distances between

Tinhosa Grande and Príncipe geckos and skinks. We note that the mean pairwise RAG1 distance between *T. adamastor* and *T. principensis* is 0.60%; however, one specimen had a lower quality assembled sequence, which caused artefactual and ambiguous base pair calls and increased the mean pairwise distance for this pairwise comparison. Additionally, the RAG-1 species delimitation analyses resulted in the grouping of several taxa that were recognised as distinct in the other gene mPTP analyses; this is most likely due to mPTP being a tree-based process and RAG-1 having a less resolved gene tree than the mitochondrial genes. These results have important taxonomic implications, especially for our current understanding of the number of species that occur in São Tomé and Príncipe as a whole. Based on our results, *T. principensis* is a junior synonym of *T. adamastor*, and *T. adamastor* should no longer be considered a Tinhosa Grande islet endemic, but a species comprising two populations, one on Príncipe and another on Tinhosa Grande. It could be argued, following the recent interpretation of the subspecies concepts by Kindler and Fritz (2018) that these two population are in fact subspecies. The arguments in favour of this interpretation are that the two population show morphological differences, are allopatric (at least currently), and exhibit limited molecular distinctiveness, and therefore these two populations may represent a case of incipient speciation (Kindler and Fritz 2018). Furthermore, as noted by Hawlitschek et al. (2012) and Kindler and Fritz (2018), the adoption of subspecies concepts may be helpful for the communication of science and conservation. Although we recognise the validity of these arguments, we refrain from adopting the subspecies concept. This decision is based on two main arguments: 1) the genetic differentiation is very minimal and we did not use any kind of analyses (such as microsatellites or population structure analyses) that would fully support their molecular distinctiveness; and 2) whether the observed pattern of sea-level changes is maintained in the future, Tinhosa and Príncipe will again be connected, and population admixture is expected. Further research on the topic may yield new data that allow different interpretations, but for now we opt to consider the skink and gecko Tinhosa Grande populations as conspecific with those of Príncipe Island.

Ceríaco (2015) and Ceríaco et al. (2016) considered the Tinhosa Grande skink as a different taxon from those of Príncipe because of its differences in body size, colouration and meristic data. These differences were comparable with those found between other congeners (see, for example, Marques et al. 2019). Although our molecular results unambiguously show that, for the present case, these characters do not reflect the genetic distinctiveness of the two populations. Phenotypic changes are important drivers of speciation in vertebrates (Rabosky et al. 2013) and have been reported to occur in lizards at an extremely rapid pace in island contexts (Amorim et al. 2017; Donihue et al. 2018; Senczuk et al. 2018). However, morphological and molecular diversifications are not necessarily correlated, with cases showing that rapid molecular diversification can occur with little morphological change and *vice versa* (Adams et al. 2009; Brawand et al. 2014). As we opted to follow a more conservative and integrative interpretation of taxonomy, in which for any taxonomic entity to be recognised would require both morphological and molecular differences, even if small (Hawlitschek et al. 2012; Kindler and Fritz 2018; Hillis 2019, 2020), the Tinhosa island populations are therefore considered conspecifics with the Principe counterparts. Habitat differences in island systems can act as selective pressures driving rapid morphological and ecological divergence in reptiles, even without any tangible genetic divergence (Vitt et al. 1997; Luiselli et al. 2005;

Bauer et al. 2012; Sagonas et al. 2013, 2014). The differences between Tinhosa Grande, an exposed rock islet, and Príncipe, covered with dense tropical vegetation (Figure 5), likely played a role in shaping the observed morphological divergence, as this has already been observed in other insular systems (Senczuk et al. 2018).

Acknowledgments

ORCID

Luis Mp Ceríaco 🄳 http://orcid.org/0000-0002-0591-9978
Justin Bernstein 🄳 http://orcid.org/0000-0002-5249-3340
Ana C Sousa 🄳 http://orcid.org/0000-0003-3435-8775
Mariana P Marques 🄳 http://orcid.org/0000-0002-1712-2632
Aaron M Bauer 🄳 http://orcid.org/0000-0001-6839-8025
Sietze J Norder 🄳 http://orcid.org/0000-0003-4692-4543

References

Adams DC, Berns CM, Kozak KH, Wiens JJ. 2009. Are rates of species diversification correlated with rates of morphological evolution? Proc. R. Soc. B. 276(1668):2729–2738.

Ali JR, Aitchison JC. 2014. Exploring the combined role of eustasy and oceanic island thermal subsidence in shaping biodiversity on the Galápagos. J Biogeogr. 41(7):1227–1241.

Aljanabi S, Martinez I. 1997. Universal and rapid salt-extraction of high quality genomic DNA for PCR-based techniques. Nucleic Acids Res. 25(22):4692–4693.

Amorim ME, Schoener TW, Santoro GRCC, Lins ACR, Piovia-Scott J, Brandão RA. 2017. Lizards on newly created islands independently and rapidly adapt in morphology and diet. Proc Natl Acad Sci USA. 114(33):8812–8816.

Bauer AM, Jackman TR, Sadlier RA, Whitaker AH. 2012. Revision of the giant geckos of New Caledonia (Reptilia: Diplodactylidae: *Rhacodactylus*). Zootaxa. 3404(1):1–52.

Bauer AM, de Silva A, Greenbaum E, Jackman T. 2007. A new species of day gecko from high elevation in Sri Lanka, with a preliminary phylogeny of Sri Lankan *Cnemaspis* (Reptilia, Squamata, Gekkonidae). Zoosyst Evol. 83 S1:22–32.

Bell RC. 2016. A new species of *Hyperolius* (Amphibia: Hyperoliidae) from Príncipe Island, Democratic Republic of São Tomé and Príncipe. Herpetologica. 72(4):343–351.

Bell RC, Parra JL, Badjedjea G, Barej MF, Blackburn DC, Burger M, Channing A, Dehling JM, Greenbaum E, Gvoždík V, et al. 2017. Idiosyncratic responses to climate-driven forest fragmentation and marine incursions in reed frogs from Central Africa and the Gulf of Guinea Islands. Mol Ecol. 26(19):5223–5244.

Bintanja R, van de Wal RSW, Oerlemans J. 2005. Modelled atmospheric temperatures and global sea levels over the past million years. Nature. 437(7055):125–128.

Bintanja R, van de Wal RSW. 2008. North American ice-sheet dynamics and the onset of 100,000-year glacial cycles. Nature. 454(7206):869–872.

Bouckaert R, Heled J, Kühnert D, Vaughan T, Wu CH, Xie D, Suchard MA, Rambaut A, Drummond AJ. 2014. BEAST 2: a software platform for Bayesian evolutionary analysis. PLOS Comput Biol. 10(4): e1003537.

Bouckaert RR, Drummond AJ. 2017. bModelTest: Bayesian phylogenetic site model averaging and model comparison. BMC Evol Biol. 17(1):42.

Brawand D, Wagner CE, Li YI, Malinsky M, Keller I, Fan S, Simakov O, Ng AY, Lim ZW, Bezault E, et al. 2014. The genomic substrate for adaptative radiation in African cichlid fish. Nature. 513 (7518):375–381.

de Bruyn M, Stelbrink B, Morley RJ, Hall R, Carvalho GR, Cannon CH, Van Den Bergh G, Meijaard E, Metcalfe I, Boitani L, et al. 2014. Borneo and Indochina are major evolutionary hotspots for Southeast Asian biodiversity. Syst Biol. 63(6):879–901.

Ceríaco LMP. 2015. Lost in the middle of the sea, found in the back of the shelf: A new giant species of *Trachylepis* (Squamata: Scincidae) from Tinhosa Grande islet, Gulf of Guinea. Zootaxa. 3973 (3):511–527.

Ceríaco LMP, Marques MP, Bauer AM. 2016. A review of the genus *Trachylepis* (Sauria: Scincidae) from the Gulf of Guinea, with descriptions of two new species in the *Trachylepis maculilabris* (Gray, 1845) species complex. Zootaxa. 4109(3):284–314.

Ceríaco LMP, Marques MP, Schmitz A, Bauer AM. 2017. The 'Cobra-preta' of São Tomé Island, Gulf of Guinea, is a new species of *Naja Laurenti*, 1768 (Squamata: elapidae). Zootaxa. 4324(1):121–141.

Ceríaco LMP, Marques MP, Bauer AM. 2018. Miscellanea Herpetologica Sanctithomae, with a provisional checklist of the terrestrial herpetofauna of São Tomé, Príncipe and Annobon islands. Zootaxa. 4387(1):91–108.

Ceríaco LMP, Agarwal I, Marques MP, Bauer AM. 2020. A review of the genus *Hemidactylus* Goldfuss, 1820 (Squamata: Gekkonidae) from Angola, with the description of two new species. Zootaxa. 4746(1):1–71.

Charles KL, Bell RC, Blackburn DC, Burger M, Fujita MK, Gvoždík V, Jongsma GFM, Kouete MT, Leaché AD, Portik DM. 2018. Sky, sea, and forest islands: Diversification in the African leaf-folding frog *Afrixalus paradorsalis* (Anura: Hyperoliidae) of the Lower Guineo-Congolian rain forest. J Biogeogr. 45(8):1781–1794.

Cutler KB, Edwards RL, Taylor FW, Cheng H, Adkins J, Gallup CD, Cutler PM, Burr GS, Bloom AL. 2003. Rapid sea-level fall and deep-ocean temperature change since the last interglacial period. Earth Planet Sci Lett. 206(3-4):253–271.

Donihue CM, Herrel A, Fabre A-C, Kmath A, Geneva AJ, Schoener TW, Kolbe JJ, Losos JB. 2018. Hurricane-induced selection on the morphology of an island lizard. Nature. 560(7716):88–91.

Fernández-Palacios JM. 2016. Island biogeography: shaped by sea-level shifts. Nature. 532(7597):42–43.

Fernández-Palacios JM, Rijsdijk KF, Norder SJ, Otto R, de Nascimento L, Fernández-Lugo S, Tjørve E, Whittaker RJ. 2016. Towards a glacial-sensitive model of island biogeography. Glob Ecol Biogeogr. 25(7):817–830.

Flantua S, Payne D, Borregaard MK, Beierkuhnlein C, Steinbauer MJ, Dullinger S, Essl F, Irl SDH, Kienle D, Kreft H, et al. 2020. Snapshot isolation and isolation history challenge the analogy between mountains and islands used to understand endemism. Glob Ecol Biogeogr. 29(10):1651–1673.

GEBCO. 2014. General Bathymetric Chart of the Oceans (GEBCO): Gridded bathymetric data sets are global terrain models for ocean and land. A global 30 arc-second interval grid. http://www.gebco.net. [Accessed 18 March 2015].

Gillespie RG, Roderick GK. 2014. Geology and climate drive diversification. Nature. 509(7500):297–298.

Hawlitschek O, Nagy ZT, Glaw F. 2012. Island evolution and systematic revision of Comoran snakes: why and when subspecies still make sense. PLoS One. 7(8):e42970.

Heaney LR, Walsh JS, Peterson AT. 2005. The roles of geological history and colonization abilities in genetic differentiation between mammalian populations in the Philippine archipelago. J Biogeogr. 32(2):229–247.

Hillis DM. 2019. Species delimitation in herpetology. J Herpetol. 53(1):3–12.

Hillis DM. 2020. The detection and naming of geographic variation within species. Herpetol Rev. 51 (1):52–56.

Jesus J, Brehm A, Harris DJ. 2005. Phylogenetic relationships of *Hemidactylus* geckos from the Gulf of Guinea islands: patterns of natural colonization's and anthropogenic introductions estimated from mitochondrial and nuclear DNA sequences. Mol Phylogenet Evol. 34(3):480–485.

Kapli P, Lutteropp S, Zhang J, Kobert K, Pavlidis P, Stamatakis A, Flouri T. 2017. Multi-rate Poisson tree processes for single-locus species delimitation under maximum likelihood and Markov chain Monte Carlo. Bioinformatics. 33:1630–1638.

Kearse M, Moir R, Wilson A, Stones-Havas S, Cheung M, Sturrock S, Buxton S, Cooper A, Markowitz S, Duran C, et al. 2012. Geneious Basic: an integrated and extendable desktop software platform for the organization and analysis of sequence data. Bioinformatics. 28(12):1647–1649.

Kindler C, Fritz U. 2018. Phylogeography and taxonomy of the barred grass snake (*Natrix helvetica*), with a discussion of the subspecies category in zoology. Vertebr Zool. 68(3):269–281.

Kumar S, Stecher G, Tamura K. 2016. MEGA7: molecular evolutionary genetics analysis version 7.0 for bigger datasets. Mol Biol Evol. 33(7):1870–1874.

Lambeck K, Rouby H, Purcell A, Sun Y, Sambridge M. 2014. Sea level and global ice volumes from the Last Glacial Maximum to the Holocene. Proc Natl Acad Sci USA. 111(43):15296–15303.

Lee D-C, Halliday AN, Fitton JG, Poli G. 1994. Isotopic variations with distances and time in the volcanic islands of the Cameroon line. Earth Planet Sci Lett. 123:119–139.

Luiselli L, Filippi E, Capula M. 2005. Geographic variation in diet composition of the grass snake (*Natrix natrix*) along the mainland and an island of Italy: the effects of habitat type and interference with potential competitors. Herpetol J. 15:221–230.

Macey JR, Larson A, Ananjeva NB, Fang Z, Papenfuss TJ. 1997. Two novel gene orders and the role of light-strand replication in rearrangement of the vertebrate mitochondrial genome. Mol Biol Evol. 14(1):91–104.

Miller EC, Sellas AB, Drewes RC. 2012. A new species of *Hemidactylus* (Squamata: Gekkonidae) from Príncipe Island, Gulf of Guinea, West Africa with comments on the African–Atlantic clade of *Hemidactylus* geckos. Afr J Herpetol. 61(1):40–57.

Norder SJ, Baumgartner JB, Borges PAV, Hengl T, Kissling WD, Van Loon EE, Rijsdijk KF. 2018. A global spatially explicit database of changes in island palaeo-area and archipelago configuration during the late Quaternary. Glob Ecol Biogeogr. 27(5):500–505.

Norder SJ, Proios K, Whittaker RJ, Alonso MR, Borges PAV, Borregaard MK, Cowie RH, Florens FBV, de Frias Martins AM, Ibáñez M, et al. 2019. Beyond the Last Glacial Maximum: island endemism is best explained by long-lasting archipelago configurations. Glob Ecol Biogeogr. 28(2):184–197.

Palumbi SR, Martin AP, Romano S, McMillan WO, Stice L, Grabowski G. 1991. The Simple Fool's Guide to PCR. Department of Zoology Special Publication. Honolulu: University of Hawaii at Manoa.

Papadopoulou A, Knowles LL. 2017. Linking micro- and macroevolutionary perspectives to evaluate the role of Quaternary sea-level oscillations in island diversification. Evolution. 17(12):2901–2917.

Portik DM, Bauer AM, Jackman TR, Portik DM, Bauer AM, Jackman TR. 2010. Phylogenetic Affinities of *Trachylepis sulcata nigra* and the Intraspecific Evolution of Coastal Melanism in the Western Rock Skink. Afr Zool. 45(2):147–159.

Rabosky DL, Santini F, Eastman J, Smith SA, Sidlauskas B, Chang J, Alfaro ME. 2013. Rates of speciation and morphological evolution are correlated across the largest vertebrate radiation. Nat Commun. 4(1):1958.

Rambaut A, Drummond AJ, Xie D, Baele G, Suchard MA. 2018. Posterior summarisation in Bayesian phylogenetics using Tracer 1.7. Syst Biol. 67(5):901–904.

Rijsdijk KF, Hengl T, Norder SJ, Otto R, Emerson BC, Ávila SP, López H, van Loon EE, Tjørve E, Fernández-Palacios JM. 2014. Quantifying surface-area changes of volcanic islands driven by Pleistocene sea-level cycles: biogeographical implications for the Macaronesian archipelagos. J Biogeogr. 41(7):1242–1254.

Sagonas K, Valakos ED, Pafilis P. 2013. The impact of insularity on the thermoregulation of a Mediterranean lizard. J Therm Biol. 38(8):480–486.

Sagonas K, Pafilis P, Lymberakis P, Donihue CM, Herrel A, Valakos ED. 2014. Insularity affects heads morphology, bite force and diet in a Mediterranean lizard. Biol J Linn Soc Lond. 112(3):469–484.

Senczuk G, Colangelo P, Avramo V, Castiglia R, Bohme W, Corti C. 2018. A study in Scarlett: incipient speciation, phenotypic differentiation and conservation implications of the *Podarcis* lizards of the western Pontine Islands, Italy. Biol J Linn Soc Lond. 125(1):50–60.

Smith SA, Sadlier RA, Bauer AM, Austin CC, Jackman T. 2007. Molecular phylogeny of the scincid lizards of New Caledonia and adjacent areas: evidence for a single origin of the endemic skinks of Tasmantis. Mol Phylogenet Evol. 43(3):1151–1166.

Uyeda JC, Drewes RC, Zimkus BM. 2007. The California Academy of Sciences Gulf of Guinea Expeditions (2001, 2006) VI. A new species of *Phrynobatrachus* from the Gulf of Guinea Islands and reanalysis of *Phrynobatrachus dispar* and *P. feae* (Anura: phrynobatrachidae). Proc Calif Acad Sci. 58:367–385.

Vitt LJ, Caldwell JP, Zani PA, Titus TA. 1997. The role of habitat shift in the evolution of lizard morphology: evidence from tropical *Tropidurus*. Proc Natl Acad Sci USA. 94(8):3828–3832.

Weigelt P, Steinbauer MJ, Cabral JS, Kreft H. 2016. Late Quaternary climate change shapes island biodiversity. Nature. 532(7597):99–102.

Weinell J, Branch WR, Colston TJ, Jackman TR, Kuhn A, Conradie W, Bauer AM2019. . A species-level phylogeny of *Trachylepis* (Scincidae: Mabuyinae) provides insight into their reproductive mode evolution. Mol Phylogenet Evol. 136:183–195.

Weisrock DW, Macey JR, Ugurtas IH, Larson A, Papenfuss TJ. 2001. Molecular phylogenetics and historical biogeography among salamandrids of the 'true' salamander clade: rapid branching of numerous highly divergent lineages in *Mertensiella luschani* associated with the rise of Anatolia. Mol Phylogenet Evol. 18(3):434–448.

Woodruff DS. 2010. Biogeography and conservation in Southeast Asia: how 2.7 million years of repeated environmental fluctuations affect today's patterns and the future of the remaining refugial-phase biodiversity. Biodivers Conserv. 19(4):919–941.